Numerical poroelastic amplitude modeling

Steven Kim* and Kris Innanen
smkim@ucalgary.ca

Introduction

Amplitude modeling is an important aspect of analyzing seismic data. These amplitudes have been studied extensively for elastic layer models in the geophysical community. Recently published work by Russell, Gray, and Hampson extends these elastic models to include poroelasticity where a quantifiable fluid term is described in the target layer. This fluid term is explicitly shown in a linearized AVO approximation. Where this approximation is derived from the Aki and Richards approximation, we have derived a linear poroelastic AVO approximation that is arguably the same as Russell and Gray's approximation. With our method, we also extend our amplitude modeling methods into the non-linear domain where higher order correcting terms shows improvement relative to the linear approximation. These expressions are detailed in this year's CREWES Report titled "*Characterization of poroelastic targets for P- and S-waves using linear and non-linear AVO methods*".

Forward amplitude modeling

Figures 1 and 2 demonstrate visual comparisons of the Zoeppritz equations and the 1st, 2nd, and 3rd order poroelastic approximations. The left column models amplitudes based on the perturbation series while the right column uses the reflectivity series. Figure 1 uses small values for perturbation modeling and figure 2 uses an incrementally higher value to emphasize a decrease in amplitudes of the linear approximations relative to the non-linear forms.

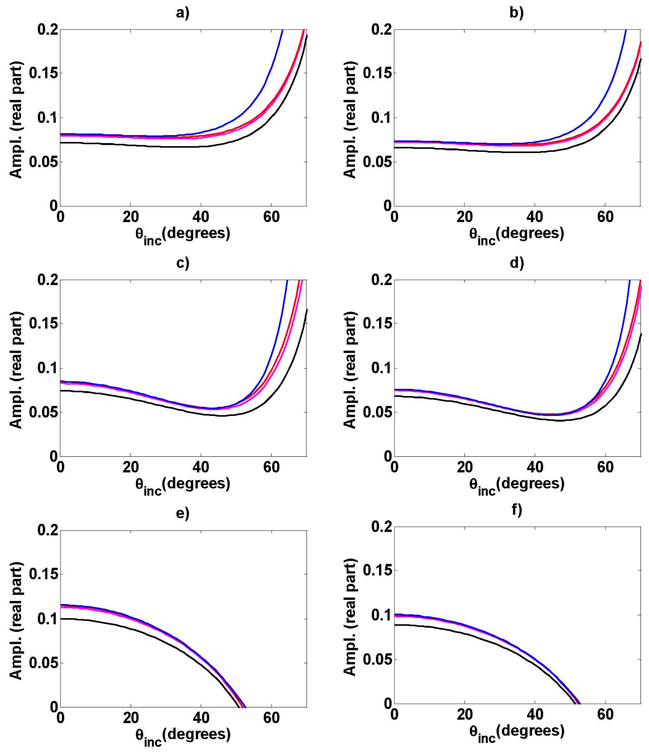

Fig 1: Linear and non-linear poroelastic amplitude approximations are shown with respect to the Zoeppritz equations. First order is shown in black, 2nd order in magenta, 3rd order in red, and Zoeppritz in blue. Table 1 indicates what model parameter values are used.

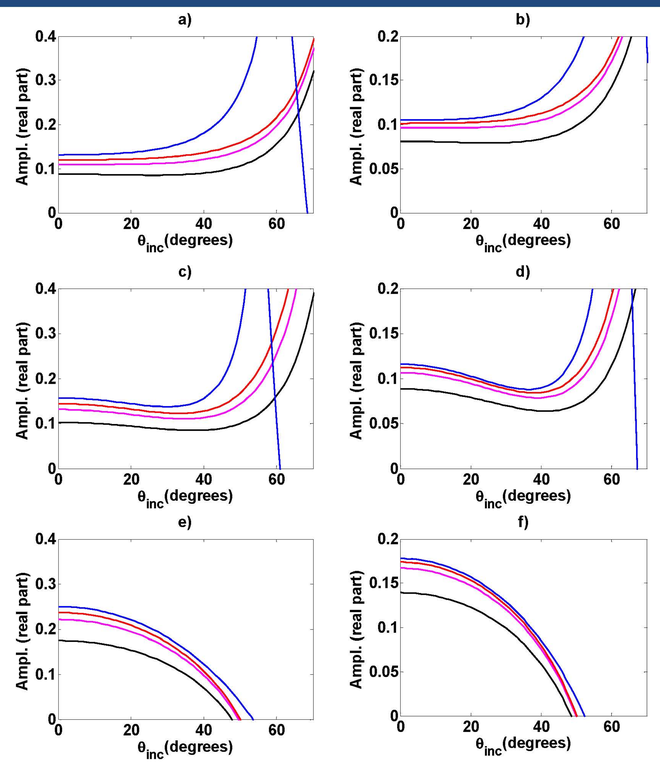

Fig 2: This figure shows larger differences in amplitudes of the approximations relative to Zoeppritz.

Inverse amplitude modeling

These inversion results are predicted using the linear approximation which solve for the fluid perturbation (a_f). The following figures are normalized residuals of known perturbation models and their estimations. Figure 3 demonstrates constant increases in magnitude of all 3 perturbation models while figures 4 and 5 show independently varying models in fluid and shear modulus respectively.

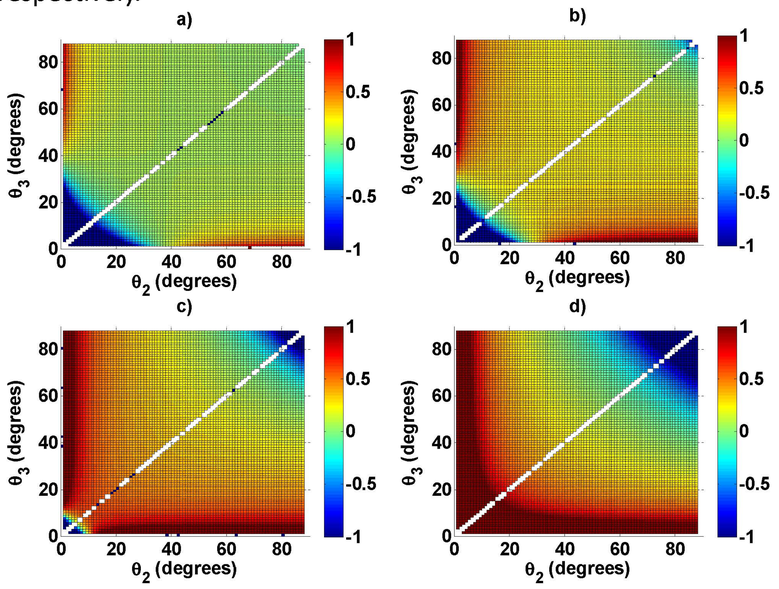

Fig 3: Plots of residual normalized linear inversions using perturbation models (a_f, a_μ, a_ρ). All three perturbation models are equal for each subfigure and demonstrate increasingly unstable results for large θ_2 and small θ_3 and vice versa.

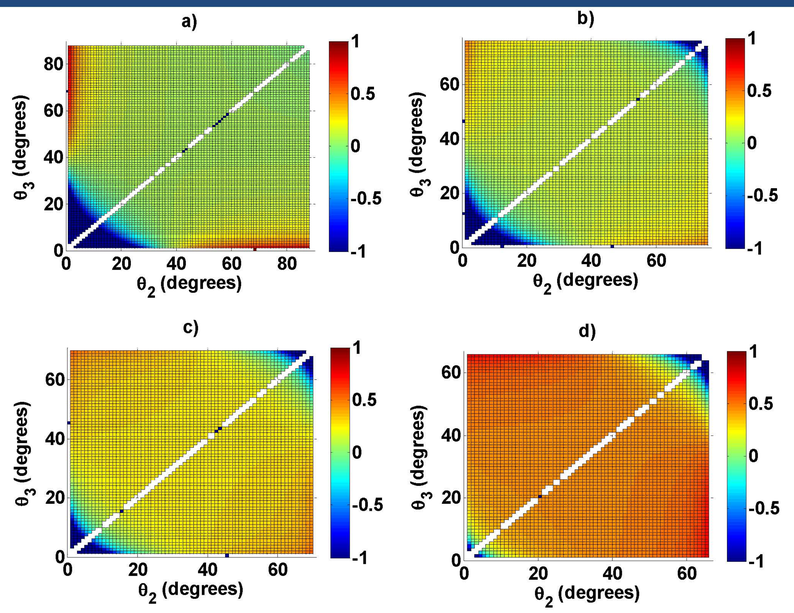

Fig 4: This figure shows linear inversion plots as figure 3 but instead uses constant a_μ and a_ρ while a_f steadily increases in equal increments. The fluid perturbation value in d) is 0.4.

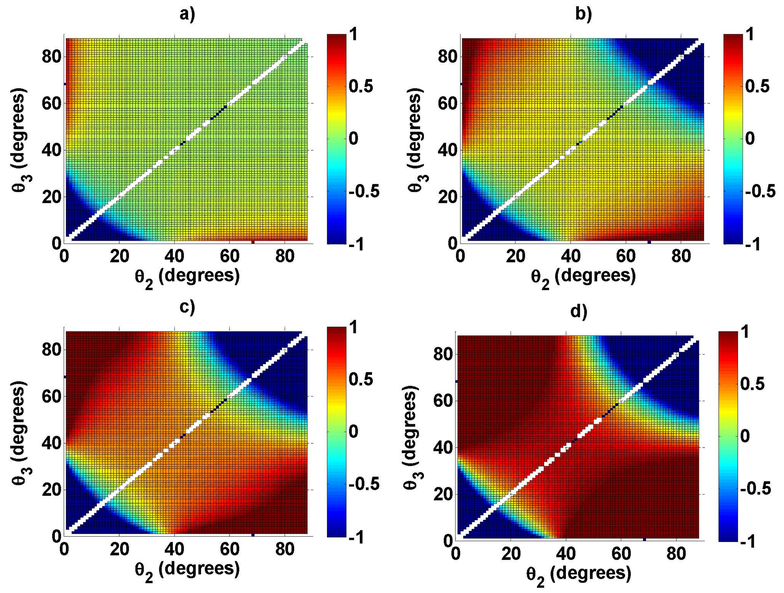

Fig 5: An estimation of the fluid perturbation parameter using an incremental increase in a_μ while a_f and a_ρ remain constant.

Conclusion

In the forward modeling results, more accuracy is achieved for higher order approximations. Inverse modeling results show zones of reflection data that are undesired for various perturbation model examples.

Acknowledgments

This work was funded by the CREWES Project and a University Research Award from Imperial Oil Limited. The authors gratefully acknowledge this support. We thank Brian Russell for valuable commentary and suggestions.